

The ultrafast photochemical ring-opening reaction of 1,3-cyclohexadiene in cyclohexane

Stuart H. Pullen, Neil A. Anderson, Larry A. Walker II, and Roseanne J. Sension
Department of Chemistry, University of Michigan, Ann Arbor, Michigan 48109-1055

(Received 21 July 1997; accepted 1 October 1997)

The ring-opening reaction of 1,3-cyclohexadiene in cyclohexane solution and the subsequent photoproduct cooling dynamics have been investigated by using two-color transient absorption kinetic measurements and novel time-resolved absorption spectroscopy in the 260–300 nm spectral region. The initial photoproduct in this reaction, *s-cis,Z,s-cis*-1,3,5-hexatriene (cZc-HT) is formed on a ~ 250 fs time scale. Spectra deduced for time delays very close to zero, as well as calculated Rice–Ramsperger–Kassel–Marcus unimolecular reaction rates, provide strong evidence that the quantum yield for the reaction is determined *before* any relaxation occurs on the ground state. Upon formation, the vibrationally excited hexatriene photoproduct is able to isomerize around C–C single bonds freely. As a result, the evolution observed in the transient absorption measurements represents a combination of rotamer population dynamics and thermalization due to energy transfer to the solvent. Three distinct time scales for relaxation are observed. These time scales correspond approximately to the development of an evolving equilibrium of Z-HT rotamers (1–5 ps), vibrational cooling and thermal equilibration with the surroundings (10–20 ps), and activated isomerization of trapped cZt-HT to tZt-HT (≥ 100 ps). © 1998 American Institute of Physics. [S0021-9606(98)01902-3]

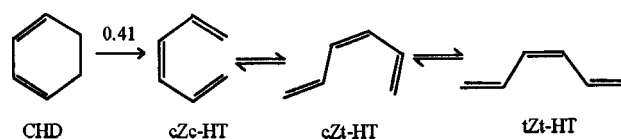
I. INTRODUCTION

The importance of polyene photochemistry in biology has long been recognized. Nature has found many intriguing ways to utilize conjugation in order to control and direct the chemistry of the natural world, from harvesting energy to restricting molecular shape. Our ability to understand the photochemistry of polyenes is then central to our understanding of some of the most fundamental reactions occurring in nature. One such example is found in the series of reactions relevant to vitamin D chemistry.^{1–3} Both ring-opening and *cis*–*trans* isomerization are important in this system.

In order to understand the fundamental processes determining the outcome of the reactions we observe in nature, it is often useful to examine the functional sub-units of complex biological systems in detail. In this case, the ring opening reaction of 1,3-cyclohexadiene (CHD) to form *cis*-1,3,5-hexatriene (Z-HT) with a 40% quantum yield⁴ is analogous to the formation of previtamin D from 7-dehydrocholesterol.¹ The study of systems with fewer degrees of freedom in many cases simplifies the interpretation of experimental data, and allows a direct comparison with theoretical calculations not always possible in the larger systems.

The absorption spectrum of CHD is characterized by the fully allowed $1^1A_1 \rightarrow 1^1B_2$ transition (see Fig. 1). Molecules excited to the 1^1B_2 state undergo a rapid radiationless decay in 10 fs.⁵ Internal conversion to a slightly lower-lying 2^1A_1 state is believed to be responsible for the ultrafast 1^1B_2 depopulation. Finally, nonradiative decay to the ground state results in photoproduct formation. Formation of the ground state photoproduct has been observed by time-resolved resonance Raman and absorption studies in the solution phase^{6–13} and by time-resolved ionization in the gas phase.¹⁴

Several recent studies indicate that the CHD ring-opening reaction occurs in less than 1 ps,^{10–14} initially producing vibrationally excited *di-s-cis*-Z-hexatriene (cZc-HT), which then isomerizes around the C–C single bonds to form more energetically favorable rotamers, *mono-s-trans* (cZt-HT) and *di-s-trans*-Z-hexatriene (tZt-HT) according to scheme 1.



The analysis of this reaction is, however, greatly complicated by the effects of vibrational excitation and a lack of information about the spectra of the two higher energy rotamers of Z-hexatriene, cZc- and cZt-HT.

Extensive work on substituted trienes has demonstrated a trend toward lower oscillator strengths and broader absorption spectra for the less stable hexatriene conformers when compared with the spectra of tEt and tZt-HT.^{2,3,15,16} Although broadening of the absorption spectrum increases the relative contributions of cZc and cEc or cZt and cEt at long wavelengths, little evidence is found for a substantial shift in λ_{\max} when comparing absorption spectra of similar systems.^{15,16} Most of these studies have compared spectra of different molecules constrained to the *di-s-cis* or *mono-s-cis* conformations by steric interactions or by specific bonds. Photochemical yield measurements can be used to confirm these trends in different rotamers of an individual molecule. In a study of a minimally substituted triene (Z-2,5-dimethyl-1,3,5-hexatriene in *n*-heptane) Brouwer *et al.* demonstrated a strong wavelength dependence for the

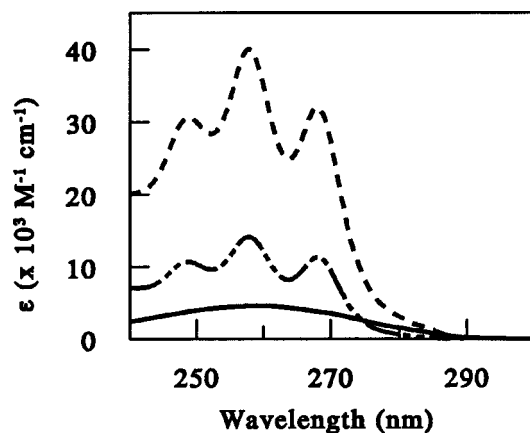


FIG. 1. Comparison of the absorption spectrum of CHD (solid line) to Z-HT (dashed line). The dashed/dotted line is the static difference assuming 40% Z-HT production from excitation of CHD.

quantum yield of the ring-closure reaction ranging from $\phi = 0.42$ at 303 nm to $\phi = 0.014$ at 248 nm.¹⁵ The wavelength dependence of the ring-closure reaction is attributed to selective excitation of the cZc rotamer on the red-edge of the absorption spectrum.

We have recently published an ultrafast transient absorption study of the internal conversion and conformational relaxation of Z-HT in cyclohexane following excitation into the strongly allowed 1^1B_2 state.¹⁷ These measurements demonstrate the recovery of vibrationally hot ground state hexatriene on a time scale of ~ 200 fs. The subsequent multiexponential relaxation is interpreted in terms of an evolving equilibrium of Z-HT rotamers and energy transfer to the surroundings (thermalization). Vibrational cooling results in the trapping of a small amount ($\sim 8\%$) of cZt-HT. The trapped cZt-HT relaxes to tZt-HT on a much longer time scale as the barrier to single-bond rotation becomes important. An estimate of the absorption spectrum of cZt-HT was obtained from the difference spectrum observed for a time delay of 50 ps. The cZt-HT spectrum is somewhat weaker and redshifted with respect to the absorption spectrum of tZt-HT as expected from the aforementioned work on substituted trienes.

In the present paper our studies of polyene dynamics are extended to investigate the ring-opening reaction of CHD. In order to investigate the dynamics of CHD after ultraviolet excitation, we have recorded time-resolved difference spectra and pump-probe kinetic traces between 263 and 300 nm. These measurements demonstrate the formation of photoproduct on a circa 250 fs time scale, and provide convincing evidence of picosecond rotational isomerization between the three isomers of Z-hexatriene following product formation. The results presented here indicate a complex and dynamic cooling process, which is very different from the step-wise process of transformation from cZc-HT to tZt-HT that one might assume *a priori*.

II. EXPERIMENT

The laser system used to perform these experiments has been described in detail previously.¹⁸ A titanium:sapphire

oscillator is amplified producing a pulse train at a repetition rate of 1 kHz, with pulses of 70 fs duration, 400 μJ pulse energy, and a central wavelength of ~ 800 nm.

Two different types of pump-probe experiments are described in this paper. Kinetic measurements at specific probe wavelengths were used to accurately determine the time dependence of the absorption changes. To facilitate accurate wavelength comparisons, transient difference spectra were also recorded at selected time delays using an ultraviolet continuum probe pulse generated by focusing the third harmonic of the laser into a sapphire window. In all cases the samples were pumped with the third harmonic, at ~ 270 nm. The experimental setup for these experiments has been described in detail elsewhere.¹⁷ 1,3-cyclohexadiene (Aldrich C10,000-5) was used as received with no further purification. Samples were diluted to an optical density (OD) of ~ 1 at 268 nm with cyclohexane (Aldrich 99+ % spectrophotometric grade). In all of the experiments, the sample was flowed through a 1 mm path length quartz cell to refresh the volume between laser pulses. The sample temperature was kept constant at 13.2 $^\circ\text{C}$ by placing the reservoir in a refrigerated bath, and the reservoir volume was replaced periodically to prevent spurious signals due to the accumulation of photoproducts.

A. Kinetics measurements

Briefly, the output from the Ti:sapphire laser was split into two beams with a 60–40 beam splitter, and used to pump both an OPA (60%) and a frequency tripler (40%). The OPA used in the kinetics experiments was pumped at 800 nm, producing tunable infrared pulses.¹⁹ This beam was then frequency doubled twice to produce tunable ultraviolet probe pulses for two-color experiments. The third harmonic of the Ti:sapphire laser, at ~ 270 nm, was used as the pump beam. The excitation pulse was ~ 150 fs in duration with an average energy of 1 $\mu\text{J}/\text{pulse}$. Kinetics measurements were made at magic angle relative polarization between the pump and probe beams. In the present investigation measurements were made at 271 nm (one-color), 274, 278, 282, 285, and 290 nm. One-color transient absorption measurements between 262 and 273 nm were described previously.¹⁰

B. Spectral measurements

The experimental setup for recording time-resolved spectra is similar to that for the kinetics measurements. The initial beam was split with a 60–40 beam splitter. Third harmonic was generated in both arms. The pump pulses in this case had an average energy of ~ 0.5 $\mu\text{J}/\text{pulse}$. The more powerful arm was used to generate 1.0–1.5 μJ of third harmonic that was then tightly focused into a 3-mm-thick piece of sapphire (Crystal Systems). The spatial profile of the beam broke down when the sapphire was placed at the focus, resulting in continuum generation. A sample spectrum of the continuum was presented in Ref. 17. No material was present in the probe arm between the sapphire and the sample cell in order to minimize temporal broadening.

After passing through the sample the probe beam was

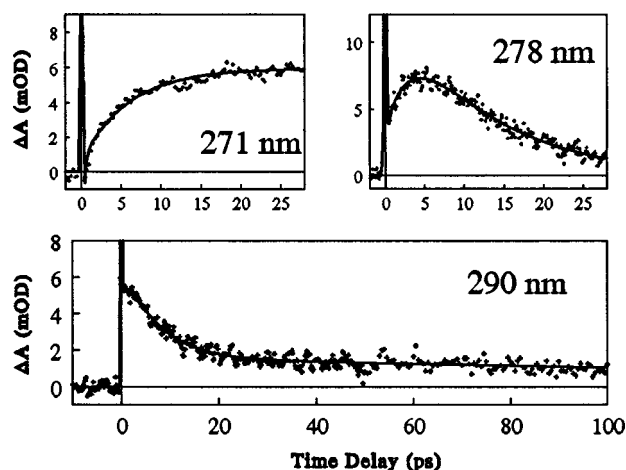


FIG. 2. Two-color kinetic measurements of CHD in cyclohexane at probe wavelengths of 278 and 290 nm as well as a one-color kinetic measurement at 271 nm. All data was collected at magic angle with an excitation wavelength of ~ 270 nm.

focused onto an optical fiber, coupling the beam into a SPEX/500M monochromator with a 1200 groove/mm diffraction grating. The detector was a Princeton Instruments liquid-nitrogen cooled charge-coupled device (CCD) camera (model LN/CCD-1100-PB). An overall resolution of 1 nm was achieved using this system.

The spectra were recorded at perpendicular relative pump and probe beam polarization so that a calcite polarizing prism placed in front of the fiber minimized detection of the pump scatter. Rotational contributions to the observed signal are small at the time delays for which we have recorded spectra. Anisotropy measurements at 262, 268, and 273 nm decay to near zero anisotropy ($|r| \leq 0.05$) within 4–5 ps. An additional anisotropy measurement of the absorbance change at 290 nm following the direct excitation of tZt-HT in cyclohexane also decays to near zero within 10 ps.¹⁷ All spectra reported here were obtained for time delays ≥ 4 ps. Hence, we have not made any correction for the difference between magic angle and perpendicular responses.

Pumped and unpumped spectra were recorded alternately by mechanically chopping the pump beam. The CCD exposure for each spectrum was 300 ms. Difference spectra were generated by averaging the base 10 logarithm of the ratio of consecutive pumped and unpumped frames. The difference spectrum reported for each time point is an average of at least 5000 pairs of spectra.

The two-photon solvent spike observed when pump and probe pulses overlap (see below and Fig. 2) was used to characterize the chirp in the UV continuum. A nonlinear ~ 1 ps chirp across the continuum (265–300 nm) was observed. In order to minimize both the effect of this chirp and of polarization on the data, spectra were obtained only for time delays ≥ 4 ps. Transient absorption spectra were obtained for time delays of 4, 5, 10, 20, 25, and 50 ps.

III. RESULTS

A. Kinetic data

Sample two-color kinetic measurements for CHD in cyclohexane, pumped at 270 nm, are shown in Fig. 2. The probe wavelengths are as indicated. A one-color measurement at 271 nm is also shown in this figure. One-color kinetic measurements between 262 and 273 nm were presented in a previous paper.¹⁰ In all of the kinetic data, there is a pulse width limited solvent absorption at zero time delay due to two-photon ionization. This is only observed at zero time delay, requiring simultaneous absorption of one pump and one probe photon for ionization to occur. This artifact has been seen in all alkane solvents we have used and for all probe wavelengths below 430 nm. In pure solvent, no further kinetic signals were observed following the spike.

The present kinetic measurements, along with the measurements reported in Ref. 10, can be fit to a model consisting of an instrument limited spike and a simple linear combination of exponentials. The fitted response is convoluted with a Gaussian instrument function whose width is determined by the solvent spike. For wavelengths longer than 273 nm, the initial rise of the transient absorption signal is approximately instrument limited. In the discussion below, this prompt long wavelength absorption is attributed to the recovery of hot ground state CHD and Z-HT. If the ground state recovery is modeled with an exponential rise, a time constant of 250 ± 100 fs is obtained for the rate of internal conversion back to the ground state of the reactant and/or product. In light of the limited temporal resolution of the present data set (instrument response of ~ 300 fs), the fit only provides an upper limit for the time scale of internal conversion.

Subsequent to the initial rise of the transient absorption signal, at least three additional exponential components are required to fit the data at most wavelengths. For example, the data at 278 nm exhibits a fast rise (≤ 250 fs), a somewhat slower picosecond rise, and a biexponential decay of the transient absorption signal (Fig. 2). Over the wavelength range studied (263–290 nm), the three exponentials obtained by fitting the data ranged from 1 to 5, 10 to 20, and > 100 ps. Neither of the two intermediate time constants were found to be wavelength independent.

The transient absorption data obtained following excitation of CHD are consistent with those reported following excitation of Z-HT.¹⁷ Vibrational relaxation in the Z-HT photoproduct is directly coupled to the population dynamics of the single-bond rotamers as well as to the evolution of the spectrum of each species. The complexity introduced by conformational relaxation precludes assignment of the observed exponential decays directly to any physical processes. The 1–5 ps component is dominated by the redistribution of Z-HT population among all three rotamers, but also contains contributions due to the overall vibrational cooling of the photoproduct. The 10–20 ps component is dominated by vibrational cooling, but also reflects more gradual shifts in rotamer populations due to decreasing isomerization rates as the system cools. The long component is attributable to a combination of the presence of the permanent photoproduct

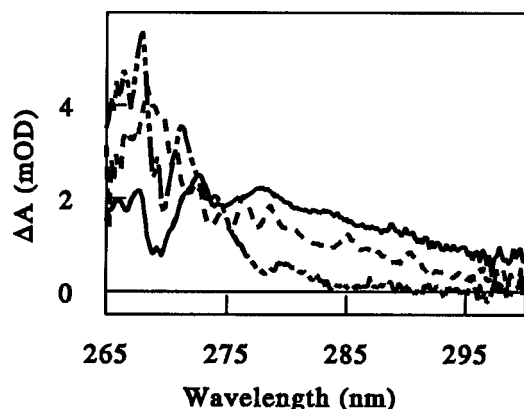


FIG. 3. Difference spectra taken at time delays of 5 ps (solid line), 10 ps (dashed line), and 25 ps (dashed/dotted line). The dip in the 5 and 25 ps spectra is due to detection of scatter from the pump beam.

and rotational isomerization of trapped cZt-HT via a thermally activated barrier crossing process.

B. Spectral data

Experimental difference spectra obtained for several time delays are presented in Fig. 3. Each spectrum has been adjusted by using a scale factor to compensate for laboratory factors such as varying pump energies and differing qualities of pump-probe overlap. A vertical offset was also used to correct for fluctuations in the baseline due to variations in the continuum intensity between pumped and unpumped frames collected by the CCD camera. These variations are small, but not negligible because the pumped and unpumped frames were not collected simultaneously. Determination of the correction factors was made by reconciling the spectral and kinetic data as described previously.¹⁷ Very good agreement between the kinetic and spectral data was achieved in this manner.

The static difference spectrum calculated by assuming a 40% Z-HT quantum yield⁴ is plotted with the absorption spectra of Z-HT and CHD in Fig. 1. CHD has a broad, structureless absorption spectrum across our spectral window, with an oscillator strength approximately one-fifth as large as that of the tZt-HT transition.¹⁸ As a result, the static difference spectrum looks like a slightly distorted tZt-HT spectrum.

The difference spectra shown in Fig. 3 clearly display the expected evolution from a very broad, mainly structureless absorption at 5 ps, to a close approximation of the static difference spectrum by 25 ps. A spectrum taken at a delay of 50 ps evidenced no significant differences from the 25 ps spectrum. Any further population dynamics after 25 ps must occur on a much longer time scale.

Dips are evident in the 5 and 25 ps spectra at ~ 270 nm due to pump scatter that was not completely eliminated even though spectra were taken with perpendicular relative polarizations.

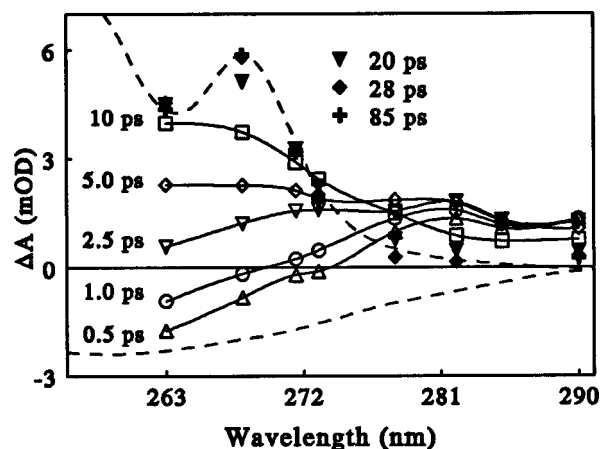


FIG. 4. Difference spectra for a series of time delays generated using the one- and two-color kinetic data. The selected time delays are indicated. The dashed lines represent the initial bleach of CHD and the static difference spectrum expected for 60% recovery of CHD and 40% formation of tZt-HT.

C. Generation of early time spectra

The corrected transient absorption spectra allow the magnitude of the kinetic measurements to be normalized so that signal intensities are not affected by differences in pump beam energy or by other experimental factors. The intensities can then be taken directly from the kinetic traces to produce a difference spectrum at any time delay. This technique is especially useful for determining the photoproduct spectrum at very early time delays. At early times, when the signal magnitude changes most rapidly, distortion due to the ~ 1 ps chirp across the spectral window would be evident in the spectra. Chirp compensation would be difficult over this broad wavelength range in the ultraviolet. Therefore, direct collection of a "1 ps spectrum" would require patching together spectra at several time points in order to approximate the same time delay for all wavelengths. It is easier and more reliable to utilize the properly scaled kinetic data for early time estimates of the difference spectrum. The solvent spike can be used to reliably locate zero for each kinetic scan, and the intensity at a desired time delay can simply be read from each scan. Close wavelength spacing of the kinetic measurements allows the data to be compiled into a spectrum. This method has been employed here to generate spectra as early as 500 fs, providing much greater insight than possible with the kinetics alone.

Difference spectra derived from the kinetic traces are shown in Fig. 4. The evolution of the difference spectrum at early times is readily apparent from the progression shown in Fig. 4. Prior to 1.5 ps, there is a bleach on the blue side of the spectrum, and no hint of the tZt-HT 0-0 band. There is, however, a substantial absorption on the red side of these spectra. Note that the magnitude of the broad absorption at 500 fs is consistent with a sub-500 fs photoproduct formation. The evidence for subpicosecond photoproduct formation is discussed in greater detail in Sec. IV. The subsequent spectral evolution in Fig. 4 illustrates the growth of the Z-HT 0-0 band, which begins to become visible at 5 ps, and develops substantially between 10 and 25 ps. The broad red absorption

grows in, peaking in intensity at about 5 ps, before declining to very little absorption at 25 ps, as expected from the spectral data.

IV. DISCUSSION

A. Subpicosecond photoproduct formation

Our earlier report indicated a rate for photoproduct formation of $>1 \text{ ps}^{-1}$ based on the fastest exponential component observed in the one-color kinetic measurements.¹⁰ The inclusion of the two-color data presented in this study allows a better estimate of $(0.25 \pm 0.1 \text{ ps})^{-1}$ from the rise of the broad redshifted absorption spectrum of the initial photoproduct. The determination of an upper limit for the internal conversion rate from the 2^1A_1 state to the 1^1A_1 state is predicated on the assumption that the broad redshifted absorption is due to the initial formation of ground state Z-HT. The possibility that an excited state absorption ($S_1 \rightarrow S_n$) could also contribute to the absorption signal cannot be ruled out entirely. However, the spectral evolution observed in Fig. 4 is most consistent with conformational and vibrational relaxation following internal conversion to the ground electronic state. The data exhibit no sign of a well-defined time constant longer than 250 fs assignable to internal conversion. This is in direct contrast to the much-studied internal conversion of *cis*-stilbene, where a clearly identifiable kinetic component assigned to decay of the S_1 excited state population is observed at wavelengths ranging from 250 nm to $>1 \mu\text{m}$ in a wide variety of solvents.²⁰

A 250 fs time scale for internal conversion to the ground state is in excellent agreement with the time-resolved gas phase ionization experiment of Trushin *et al.* which found that *cZc*-HT is formed within 200 fs.¹⁴ A subpicosecond ground state recovery is also consistent with the conical intersection mechanism for return to the ground state proposed by Robb *et al.* based on theoretical calculations of the potential energy surfaces.²¹⁻²³

The spectrum of the initial photoproduct formed following excitation of CHD can be estimated from the differences observed at 800 fs. Assuming a 40% quantum yield for the formation of Z-HT and adding back the bleach due to CHD depopulation gives the initial photoproduct spectrum shown in Fig. 5. The 800 fs photoproduct spectrum determined from the kinetic data is broad and without resolved structure, peaking at about 280 nm. The oscillator strength of the absorption due to the initial photoproduct appears to be somewhat larger than that of relaxed CHD. However, a quantitative determination of the oscillator strength of the initial photoproduct absorption is not possible with the limited spectral window available.

There is no experimental knowledge of the spectrum of *cZc*-HT, although a matrix isolation experiment on *E*-hexatriene provides some evidence that *cEc*-HT may have a broad absorption extending to 300 nm.²⁴ The spectra of *tZt* and *tEt*-hexatriene are quite similar.²⁵ The spectra of *cZt*-HT and *cEt*-HT also appear to correspond well.^{17,24} Hence, we

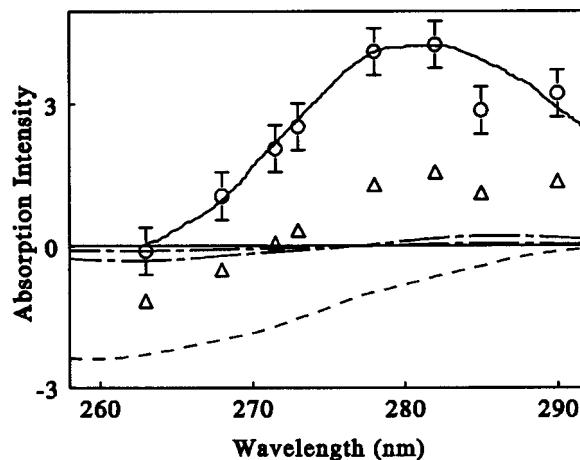


FIG. 5. An estimate of the initial Z-HT absorption spectrum. The dashed line corresponds to the bleach of CHD in the initial excitation process while the open triangles represent the experimental difference spectrum at 800 fs obtained from the kinetic data. The open circles represent the calculated spectrum of *cZc*-HT at 800 fs assuming a 40% quantum yield for formation. The error bars encompass errors due to both the determination of the 800 fs difference spectrum and the uncertainty in the hot spectrum of the initially recovered CHD. The solid line represents the spectral shape suggested by the data. The dot-dashed lines represent estimates of the CHD difference spectrum for $T=1000 \text{ K}$ and $T=2000 \text{ K}$ assuming 60% recovery of CHD.

would expect *cZc*-HT to have a weak broad spectrum, perhaps peaking somewhat to the red of the other two rotamers. A trend toward broader, weaker spectra for *cZt* and *cZc* conformers is also observed in sterically hindered trienes, as discussed in Sec. I.^{2,3,15,16} In addition, a time-resolved spectrum obtained following the photolysis of CHD vapor exhibits a peak at 280 nm attributed to vibrationally hot Z- and E-HT.²⁶ *Ab initio* calculations performed in GAUSSIAN 90²⁷ (6-31G basis set) indicate that the oscillator strength of *cZc*-HT is expected to be substantially higher than that of CHD, but lower than the other two rotamers of Z-HT.¹⁰ Relative oscillator strengths of 1.0 (*tZt*-HT), 0.55 (*cZt*-HT), 0.24 (*cZc*-HT), and 0.14 (CHD) are calculated, while a ratio of 0.19 is observed experimentally for CHD:*tZt*-HT.²⁵ These calculated trends are also consistent with trends observed comparing extinction coefficients for substituted trienes. Comparison of the absorption spectra of *E*-2,5-dimethylhexatriene (stable *tEt*) with *E*-2,5-di-*tert*-butylhexatriene (stable *cEc*) provides a ratio of 0.23 for $\epsilon_{\text{max}}(\text{cEc})$: $\epsilon_{\text{max}}(\text{tEt})$,¹⁶ while comparison of *Z*-2,5-dimethylhexatriene (stable *cZt*) and *Z*-2,5-di-*tert*-butylhexatriene (stable *cZc*)¹⁵ with *Z*-hexatriene provides relative extinction coefficients of 1.0 (*tZt*), 0.3 (*cZt*), and 0.1 (*cZc*) for the three rotamers.

The magnitude and appearance of the photoproduct absorption observed at 800 fs is consistent with the expected spectrum of *cZc*-HT. The absorption spectrum is redshifted somewhat more than expected from comparison with substituted trienes. However, the initial spectrum still provides strong evidence of photoproduct formation on an ultrafast, subpicosecond time scale.

B. *Cis*-hexatriene ground state population dynamics

Cis-hexatriene can exist as any of three rotamers. At room temperature, *tZt*-HT accounts for $\geq 98\%$ of the population. However, in the ring opening of CHD the hexatriene photoproduct must initially form as the *cZc*-HT rotamer before proceeding to form the other rotamers during vibrational cooling. Time-resolved resonance Raman studies suggested that *cZc*-HT isomerizes to *cZt*-HT on a 7 ps time scale, and that *tZt*-HT formation follows on a nanosecond time scale.^{6–9} Our earlier work on the dynamics of Z-HT following excitation has shown that the single bond rotational isomerization barriers are negligible when compared to the amount of excess energy present at early times.¹⁷ As a result, an evolving equilibrium between the three rotamers is rapidly established, during the energy randomization of the first few picoseconds. The same situation should prevail following excitation of CHD, with the only difference being the initial rotamer population. Studies of *tZt*-HT also demonstrated that a small fraction of Z-HT was trapped as *cZt*-HT for much longer than 50 ps. This trapping allowed an estimate of the spectrum of the *cZt*-HT rotamer.¹⁷

Within a few picoseconds of the excitation of CHD in cyclohexane, the experimental transient absorption signals will be dominated by a superposition of ground state CHD and Z-HT relaxation processes. Internal conversion from the excited electronic state will result in the formation of vibrationally hot CHD and Z-HT. Although recent work has shown that fast intramolecular energy randomization should not be assumed *a priori*,^{20,28–30} there is no evidence in the present data for a non-Boltzmann distribution of the excess energy. Assuming harmonic vibrations, an excitation photon at 270 nm, and a Boltzmann statistical distribution of the available excess energy among all of the available degrees of freedom, an estimate of the vibrational temperature may be made.^{17,20} Using literature values for the vibrational frequencies^{31,32} and a ΔH of 5300 cm^{-1} for the formation of *tZt*-HT from CHD,³³ the initial temperature is estimated as 2270 K for CHD and 2025 K for Z-HT. These estimates provide upper limits for the internal vibrational temperature of the initial photoproducts.

The method of Shreve and Mathies was used to estimate the absorption spectrum for both CHD and *tZt*-HT as a function of internal vibrational temperature.^{17,34} This algorithm assumes harmonic vibrations and uses coordinate displacements derived from resonance Raman data.⁵ In our previous work, calculated hot spectra for *tZt*-HT were used to model transient difference spectra obtained following direct excitation of *tZt*-HT.¹⁷

Excitation of CHD results in the production of Z-HT with a quantum yield of 0.4. The remaining 60% of the molecules initially excited return to the ground electronic state as vibrationally excited CHD. The calculated hot spectrum of CHD exhibits a drop in peak intensity and broadening as a result of vibrational excitation, however, the spectral changes are comparatively small. The difference spectra estimated for 60% recovery of CHD at internal temperatures of 1000 and 2000 K are shown in Fig. 5 along with the transient absorp-

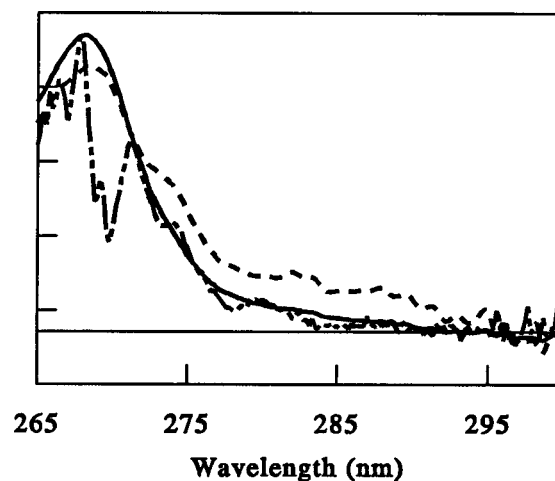


FIG. 6. The difference spectrum at 25 ps (dotted/dashed line) is well modeled by a composition of 60% CHD, 35% *tZt*-HT, and 5% *cZt*-HT (solid line). Larger quantities of *cZt*-HT result in a broad absorption on the red side of the spectrum that is not seen in the experimental data. Shown is 20% *tZt*-HT and 20% *cZt*-HT (dashed line).

tion signal observed at 800 fs. These calculations demonstrate that spectral broadening due to vibrational excitation in the CHD recovery channel will have very little effect on our observations, and therefore only the spectral evolution due to the thermalization of Z-HT need be included in the final analysis.

Once an equilibrium between Z-HT rotamers is achieved, the behavior observed following excitation of CHD will be identical to that observed following the direct excitation of Z-HT. Therefore, we postulate that 10%–15% of the Z-HT photoproduct at 50 ps exists in the *cZt*-HT rotamer, as observed in direct excitation of Z-HT. By 50 ps, the molecules have cooled enough that the rotational isomerization to form *tZt*-HT has become a barrier crossing process. Any remaining *cZt*-HT at this point could easily be trapped for hundreds of picoseconds or more by the requirement of thermal activation.

Figure 6 shows a comparison of the experimental spectrum at 25 ps to the static difference spectrum, calculated assuming a photoproduct distribution of 60% CHD, 35% *tZt*-HT, and 5% *cZt*-HT. The absorption spectrum of *cZt*-HT was determined previously, while we estimate that the *tZt*-HT has relaxed to a temperature of $\sim 550 \text{ K}$.¹⁷ For reference, a predicted spectrum is also included for a photoproduct distribution of 60% CHD, 20% *tZt*-HT, and 20% *cZt*-HT. The broad absorption, which one would expect in the spectrum of a sample containing $\geq 10\%$ *cZt*, is not observed in the 25 or 50 ps spectra. The majority of the Z-HT has relaxed to *tZt*-HT by this time. This analysis allows bounds of 0 to 6% to be set for the trapping of *cZt*-HT following excitation of CHD.

The time-resolved resonance Raman measurements of Mathies and co-workers clearly indicate the presence of *cZt*-HT at time delays of a few nanoseconds.^{6–9} Direct quantitative analysis of the *cZt*-HT population in the Raman studies is complicated by the effects of vibrational excitation at

early times, and by the fact that the experiments were performed at 282 nm, which is preresonant to tZt-HT, but is apparently in resonance with cZt-HT. Our measurements of the spectral evolution indicate that the cZt-HT population is likely to fall within the 4%–6% range after 25–50 ps. It is evident that the most consistent interpretation of the transient absorption and resonance Raman data is that a small population of cZt-HT remains at 25 ps. Having cooled significantly, this population then isomerizes to tZt-HT, by means of a thermally activated barrier crossing process, on a time scale of nanoseconds as indicated by the Raman and infrared measurements.^{6–9,35}

C. The ring-opening reaction mechanism

Theoretical studies of the excited state potential energy surfaces indicate that the ring-opening reaction of CHD occurs on the excited state surface. The conical intersection responsible for ultrafast internal conversion from the 2^1A_1 state to the 1^1A_1 ground state is calculated to have a cZc-HT configuration.²³ The 60% recovery of CHD has therefore been proposed to result from ring closure upon return to the ground state. In theory, ring closure may occur either before or after intramolecular energy redistribution within the ground state cZc-HT molecule.

In order to determine the likelihood of ring closure in the initially formed hot cZc-HT photoproduct, GAUSSIAN 94³⁶ HF/4-31G calculations were performed to characterize the expected transition state for the ground state ring-closure process. The results of these calculations indicate a barrier height of $\sim 12\,500\text{ cm}^{-1}$ for the reaction cZc-HT \rightarrow CHD, and a barrier of $\sim 20\,000\text{ cm}^{-1}$ for the back reaction. These barriers are somewhat larger than the vapor phase values of $\sim 10\,400$ and $15\,700\text{ cm}^{-1}$ reported by Orchard and Thrush.³⁷

The barriers for ring opening and ring closure are much larger than those calculated or observed for single bond rotational isomerization ($1000\text{--}3000\text{ cm}^{-1}$), but still substantially less than the $\sim 33\,000\text{--}37\,000\text{ cm}^{-1}$ initially placed into the system. The barrier is certainly low enough that either reaction could, in principle, occur on the ground state with the energy available following internal conversion from the excited electronic state. The transition state calculated above can be used along with calculated or experimental barrier heights, and the total internal energy to estimate the initial rate for formation of CHD from cZc-HT and cZc-HT from CHD. A Rice–Ramsperger–Kassel–Marcus (RRKM) calculation (performed as described in Ref. 17) suggests that the initial rate for the formation of CHD from cZc-HT would be on the order of nanoseconds to hundreds of nanoseconds, while CHD would form cZc-HT in tens of nanoseconds to microseconds. These rate constants are consistent with the observed formation of CHD following the excitation of Z-HT or E-HT in the gas phase.^{33,37} The present estimates are also consistent with a RRKM calculation performed by Cromwell *et al.* for CHD ring opening at a vibrational temperature of $\sim 3000\text{ K}$.³⁸ However, isomerization on the ground state surface is clearly not involved in the solution

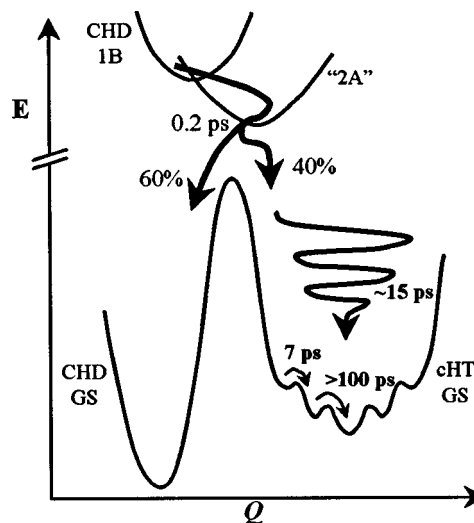


FIG. 7. A schematic diagram of the photochemical ring-opening reaction of CHD following excitation into the allowed 1^1B_2 state. The barrier heights on the ground state and the relative energies of CHD and the Z-HT rotamers are drawn to scale based on the present calculations. These are in reasonable agreement with experimental values where available.

phase photochemistry. The expected initial rate constants for ring opening or ring closure are several orders of magnitude slower than the observed rate for vibrational relaxation and equilibration with the surroundings.

Elimination of a “thermally” activated ground state isomerization pathway dictates that the observed quantum yield must result from a branching in the excited state, or a partitioning immediately upon return to the ground state as a result of the shape of the potential energy surfaces near the conical intersection. An excited state branching to form cZc-HT and CHD would require the presence of multiple crossings between the excited and ground state, one leading directly to CHD and another to Z-HT. Three intersections have been found theoretically, but only one is thought to be a viable avenue for recovery. The other two were calculated to lie substantially higher in energy.²³ Our observations lend further credence to the belief that only one intersection is involved in the reaction. Subpicosecond photoproduct formation allows very little time to cross substantial barriers and undergo the larger geometric distortions necessary to reach the other intersections.

Since multiple conical intersections are unlikely to play a role in the ring-opening reaction of CHD, we must conclude that the quantum yields for recovery of CHD and formation of Z-HT result from the nature of the ground and excited state surfaces in the immediate vicinity of the conical intersection. Momentum imparted to the molecules in the internal conversion process directs the product either to CHD or to hexatriene, while subsequent energy randomization and vibrational cooling assures that the photochemical yields are fixed.

V. CONCLUSIONS

The basic features of the CHD photochemical ring-opening reaction are illustrated in Fig. 7. Following excita-

tion, CHD returns to the ground state in ~ 250 fs, indicating that a very efficient coupling mechanism between excited and ground state, such as a conical intersection, is responsible for the internal conversion. The quantum yield for the formation of Z-HT versus the recovery of CHD is determined by the form of the conical intersection, before any relaxation or energy redistribution occurs in the ground state. The 40% Z-HT formed from the ring-opening reaction is able to undergo rotational isomerization from the sterically hindered *cZc*-HT rotamer to an evolving distribution of *cZc*-HT, *cZt*-HT, and *tZt*-HT during cooling. This evolving equilibrium of Z-HT rotamers is established on a time scale of 1–5 ps. Initially, the barriers for single bond isomerization are negligible compared to the amount of excess energy in the system. As energy is lost to the surrounding solvent, those barriers become more important, and the equilibrium favors formation of *tZt*-HT. Vibrational cooling and thermal equilibration with the surroundings occurs on a time scale of 10–20 ps. A small quantity of *cZt*-HT ($\leq 15\%$ of the Z-HT population, $\leq 6\%$ of the total CHD+Z-HT photoproduct population) may be trapped for nanoseconds by the barrier to single bond isomerization, consistent with Raman observations indicating the presence of excess *cZt*-HT at time delays of a few nanoseconds.

ACKNOWLEDGMENTS

The authors would like to thank A.-C. Tien and T. S. Sosnowski at the Center for Ultrafast Optical Science for assistance with the optimization of the generation of pump and probe pulses. The authors would also like to thank Dr. A. P. Shreve for the code to calculate hot spectra. This work is supported by a grant from the NSF (No CHE-9415772). S.H.P. is supported by the NSF through the Center for Ultrafast Optical Science, under Grant No STC PHY 8920108.

¹H. J. C. Jacobs and E. Havinga, *Adv. Photochem.* **11**, 305 (1979).

²W. G. Dauben, B. Disanayaka, D. J. H. Funhoff, B. E. Kohler, D. E. Schilke, and B. Zhou, *J. Am. Chem. Soc.* **113**, 8367 (1991).

³W. G. Dauben, E. L. McInnis, and D. M. Michno, *Rearrangements in Ground and Excited States*, edited by P. de Mayo (Academic, New York, 1980), p. 91.

⁴N. G. Minnaard and E. Havinga, *Recl. Trav. Chim. Pays-Bas.* **92**, 1315 (1973).

⁵M. O. Trulson, G. D. Dollinger, and R. A. Mathies, *J. Chem. Phys.* **90**, 4274 (1989).

⁶P. J. Reid, S. J. Doig, and R. A. Mathies, *Chem. Phys. Lett.* **156**, 163 (1989).

⁷P. J. Reid, S. J. Doig, and R. A. Mathies, *J. Phys. Chem.* **94**, 8396 (1990).

⁸P. J. Reid, S. J. Doig, S. D. Wickham, and R. A. Mathies, *J. Am. Chem. Soc.* **115**, 4754 (1993).

⁹P. J. Reid, M. K. Lawless, S. D. Wickham, and R. A. Mathies, *J. Phys. Chem.* **98**, 5597 (1995).

¹⁰S. H. Pullen, L. A. Walker II, B. Donovan, and R. J. Sension, *Chem. Phys. Lett.* **242**, 415 (1995).

¹¹S. H. Pullen, L. A. Walker II, N. A. Anderson, and R. J. Sension, *Ultrafast Phenomena X*, edited by P. Barbara, J. G. Fujimoto, W. Knox, and W. Zinth (Springer-Verlag, Berlin, 1996), p. 266.

¹²W. Fuß, T. Schikarski, W. E. Schmid, S. A. Trushin, and K. L. Kompa, *Chem. Phys. Lett.* **262**, 675 (1996).

¹³W. Fuß, W. E. Schmid, and K. L. Kompa, in Ref. 11, p. 260.

¹⁴S. A. Trushin, W. Fuß, T. Schikarski, W. E. Schmid, and K. L. Kompa, *J. Chem. Phys.* **106**, 9386 (1997).

¹⁵A. M. Brouwer, J. Cornelisse, and H. J. C. Jacobs, *Tetrahedron* **43**, 435 (1987).

¹⁶A. M. Brouwer, J. Cornelisse, and H. J. C. Jacobs, *J. Photochem. Photobiol. A* **42**, 117 (1988).

¹⁷S. H. Pullen, N. A. Anderson, L. A. Walker II, and R. J. Sension, *J. Chem. Phys.* **107**, 4985 (1997).

¹⁸S. Pullen, L. A. Walker II, and R. J. Sension, *J. Chem. Phys.* **103**, 7877 (1995).

¹⁹V. V. Yakolev, B. Kohler, and K. R. Wilson, *Opt. Lett.* **19**, 2000 (1994).

²⁰R. J. Sension, S. T. Repinec, A. Z. Szarka, and R. M. Hochstrasser, *J. Chem. Phys.* **98**, 6291 (1993).

²¹F. Bernardi, S. De, M. Olivucci, and M. A. Robb, *J. Am. Chem. Soc.* **112**, 1737 (1990).

²²P. Celani, S. Ottani, M. Olivucci, F. Bernardi, and M. A. Robb, *J. Am. Chem. Soc.* **116**, 10141 (1994).

²³P. Celani, F. Bernardi, M. A. Robb, and M. Olivucci, *J. Phys. Chem.* **100**, 19364 (1996).

²⁴Y. Furukawa, H. Takeuchi, I. Harada, and M. Tasumi, *J. Mol. Struct.* **100**, 341 (1983).

²⁵N. G. Minnaard and E. Havinga, *Recl. Trav. Chim. Pays-Bas.* **92**, 1179 (1973).

²⁶A. Kumar, P. K. Chowdhury, K. V. S. Rama Rao, and J. P. Mittal, *Chem. Phys. Lett.* **212**, 103 (1993).

²⁷GAUSSIAN 90, Revision I, M. J. Frisch *et al.*, Gaussian, Inc., Pittsburgh PA, 1990.

²⁸P. Matousek, A. W. Parker, W. T. Toner, M. Towrie, D. L. A. de Faria, R. E. Hester, and J. N. Moore, *Chem. Phys. Lett.* **237**, 373 (1995).

²⁹J. Qian, S. L. Schultz, and J. M. Jean, *Chem. Phys. Lett.* **233**, 9 (1995).

³⁰S. L. Schultz, J. Qian, and J. M. Jean, *J. Phys. Chem.* **101**, 1000 (1997).

³¹C. DiLauro, N. Neto, and S. Califano, *J. Mol. Struct.* **3**, 219 (1969).

³²R. Liu and X. Zhou, *J. Phys. Chem.* **97**, 1850 (1993).

³³S. W. Orchard and B. A. Thrush, *Proc. R. Soc. London, Ser. A* **337**, 243 (1974).

³⁴A. P. Shreve and R. A. Mathies, *J. Phys. Chem.* **99**, 7285 (1995).

³⁵E. Kauffmann, H. Frei, and R. A. Mathies, *Chem. Phys. Lett.* **266**, 554 (1997).

³⁶GAUSSIAN 94, Revision B.3, M. J. Frisch *et al.*, Gaussian, Inc., Pittsburgh PA, 1995.

³⁷S. W. Orchard and B. A. Thrush, *Proc. R. Soc. London, Ser. A* **337**, 257 (1974).

³⁸E. F. Cromwell, D.-J. Liu, M. J. J. Vrakking, A. H. Kung, and Y. T. Lee, *J. Chem. Phys.* **95**, 297 (1991).